KRONOS FUSION ENERGY

PAPER 2.1 · THE KRONOS 2026 SERIES

The Kronos Strategic-Materials Platform: An Integrated Spherical-Tokamak Breeder and D-3He Tandem-Mirror Burner Architecture with a Helium-3 Flywheel

Compact fusion is usually presented as a single machine chasing net electricity. Kronos is instead a platform of two machines with one physics record: a compact...

Read it live — 3-D model · physics validator · film series

BY P I FORD

2026 · EDITORIAL EDITION

THE OFFICIAL RECORD

What this document is, and how to read its numbers

This is a combined editorial. It gathers, in one volume, the two design studies Kronos Fusion Energy released in 2026 — a compact spherical-tokamak tritium/helium-3 breeder and a deuterium–helium-3 tandem-mirror generator — together with the intellectual-property estate, the people, and, in the internal edition, the full commercial case. The scientific text is the same text that appears in the arXiv preprints and the journal submissions; the editorial adds the apparatus a reader needs to hold the whole program at once, and nothing in the physics is altered to fit it.

THE HONESTY STANCE IS THE ASSET

Every headline quantity carries an **evidence class** — DERIVED RECOMPUTED MEASURED REQUIREMENT — and, where a number is a modelled extrapolation rather than a demonstrated value, it is labelled as such and its downside is shown next to it. Several quantities in the underlying corpus moved after first publication; where a value has been withdrawn or restated, the record says so plainly. This is deliberate: a diligence team will find the load-bearing assumptions, so the document surfaces them first.

TWO EDITIONS

This volume is issued in two editions. The **public edition** (light) carries the physics and the design only — no dollar, price, or per-kilogram figure appears anywhere in it. The **internal edition** (dark) adds the economics, the funding architecture, and the defense-commercial analysis, and is marked *Confidential* accordingly; it is not for public distribution. Where the commercial case rests on a modelled assumption rather than a demonstrated one, it is labelled as such and its downside is shown alongside it, on the same terms as the physics.

TITLE	The Kronos Fleet — Hyperion · Aegis · MetroVolt: A Combined Design & Commercialization Study
AUTHOR	Priyanca Ford, Founder & CEO, on behalf of Kronos Fusion Energy
EDITION	2026 Combined Editorial · first issue
COMPANION WORKS	The five-paper arXiv drop — (1) Breeder, (2) Burner, (3) REBCO magnet & tape, (4) Direct Energy Conversion, (5) AI/ML/Quantum control — with matching numbered Zenodo deposits, plus the IOP journal and IAEA-FEC submissions. Patents were filed before the drop.
NAMING	Hyperion = the breeder; Aegis (defense) and MetroVolt (data-center) = one generator in two housings. Internal mode letters (D1, L) do not appear on public surfaces.
STATUS	Conceptual design & simulation study. Nothing herein is a construction commitment.

HOW TO READ THIS VOLUME

The fleet at a glance, and the way its numbers are marked

This volume opens with *Orientation*, presents the five research papers as a bound sequence, and closes with the *Apparatus*. *Foundations* sets out the three general results both machines rest on. *Paper One* is the Hyperion breeder; *Paper Two* the Aegis / MetroVolt generator; *Papers Three, Four and Five* are the enabling science — high-field REBCO magnets and tape, direct energy conversion, and the AI / ML / quantum control stack. A *Digital Twin & 3-D Model* part follows, then the *Environmental* profile. The *Economics* and levelized cost and the *Business Case* and diligence record appear in the internal edition only; the *Simulations* proof record and the Apparatus — patent portfolio, team, limitations, and sources — close both editions.

THE FLEET AT A GLANCE

	HYPERION	AEGIS	METROVOLT
Role	Strategic-isotope foundry	Defense installation power	Campus power
Machine	**Spherical tokamak**	**Tandem mirror**	**Tandem mirror**
Fuel	Deuterium–tritium	Deuterium–helium-3	Deuterium–helium-3
Delivers	Tritium · ^{3}He · 14 MeV n	Resilient installation power	Firm campus power
Physics bar	**Fusion gain only**	Closure (gates named)	Closure + lunar ^{3}He
In the fleet	Breeds the fuel	Proves the generator	Commercial destination

HOW THE NUMBERS ARE MARKED

Every headline quantity carries an evidence class — DERIVED from first principles, RECOMPUTED from raw data, MEASURED in hardware, or a REQUIREMENT yet to be met. Financial figures carry a case label and are confined to the internal (confidential) edition. Values that moved after first publication are shown as withdrawn or restated rather than quietly changed. A capability you can evaluate is one whose limits are on the page.

ABSTRACT

The Kronos Strategic-Materials Platform: An Integrated Spherical-Tokamak Breeder and D-3He Tandem-Mirror Burner Architecture with a Helium-3 Flywheel

Compact fusion is usually presented as a single machine chasing net electricity. Kronos is instead a *platform* of two machines with one physics record: a compact negative-triangularity spherical-tokamak *breeder* (Hyperion) that makes strategic materials, and a deuterium–helium-3 tandem-mirror *burner* (deployed as Aegis and MetroVolt) that makes power. We give a single, self-consistent formal treatment of the platform. The breeder operates at gain $Q = 3.076$ with fusion power $P_{\text{fus}} = 85.04\,MW$ and plasma current $I_p = 9.66\,MA$ behind a 16.84 T centrepost, supplying tritium along a net breeding ladder that clears self-sufficiency ($\text{TBR}_{\text{net}} = 1.05$) and reaches an advanced ceiling of 1.42; the burner reaches engineering gain $Q_E = 1.318$ at a neutron energy fraction of only 5.44%, recovering charged-particle power through a direct converter at $\eta_{\text{DEC}} = 0.49$ behind a distinct 26.49 T plug coil. We derive the two power balances, the breeding neutronics, and—as the paper's central contribution—the *helium-3 flywheel*: a formal inventory model in which surplus tritium is banked and decays to ^{3}He with a $12.32\,yr$ half-life, so the strategic co-product is released at a rate that approaches the tritium surplus only over an e-folding time of $\tau \approx 17.8\,yr$. This slow discharge is decisive: matching a burner's $170.2\,kg\,\text{yr}^{-1}$ helium-3 demand from banked-tritium decay would require 45–192 breeders per burner, so burner-scale helium-3 does not close indigenously and is lunar-gated around 2038–40, while each breeder's $\sim$0.15--0.9$kg - T\,\text{yr}^{-1}$ of ^{3}He remains a strategic co-product rather than bulk fuel. Every headline quantity is a frozen anchor in the Kronos Physics De-Risking Register, and the whole design set was produced and independently re-run on an NVIDIA GPU high-performance-computing campaign. We state closure in two explicit tiers throughout: all three products close on the frozen physics, and the distance from closed-on-model to closed-demonstrated is a small number of named experiments, not open physics.

Open-access deposit (code & data, CC BY 4.0): DOI 10.5281/zenodo.22645764 · Zenodo community *kronos_fusion_energy*. Explore it live: interactive 3-D model · physics validator.

Keywords: fusion platform · spherical-tokamak breeder · tandem-mirror burner · helium-3 · tritium breeding · direct energy conversion · two-tier closure

CONTENTS

Table of Contents

NOMENCLATURE

Symbols, units, and the names of things

Q	plasma (fusion) gain, P_{fus}/P_{aux}
Q_E	engineering gain, net electric out / recirculating in
H_{98}	confinement enhancement over the IPB98(y,2) scaling
Z_{eff}	effective ion charge
c_{ee}	electron–electron bremsstrahlung leading coefficient, 2.120022 (exact)
τ_E	energy confinement time
I_p	plasma current
R_0, a	major radius, minor radius
κ, δ	elongation, triangularity
β_N	normalized plasma beta (Troyon-normalized)
TBR	tritium breeding ratio
DEC	direct energy conversion
CF	plant capacity factor (availability)
FOAK / NOAK / BOAK	first / n^{th} / best of a kind
Hyperion	the ST breeder (internal: Mode D2)
Aegis	the generator, defense/installation housing (internal: Mode M)
MetroVolt	the generator, data-center housing (Mode M)

§ 1

Introduction

FROM A SINGLE MACHINE TO A PLATFORM

The dominant framing of magnetic fusion is a race to net electricity from one machine. That framing has organised the field productively for decades, from the Lawson power-balance criterion [1] through the ITER physics basis [2], but it obscures a fact that the neutron economy of fusion makes plain: a deuterium–tritium plasma is, before it is a power source, a *strategic-materials factory*. A single 14 MeV neutron breeds tritium, transmutes lithium, multiplies in beryllium, and activates target nuclei into medical and industrial isotopes. Kronos is built on that observation. It is not one machine but a platform of two (figure 1): a compact spherical-tokamak *breeder* that makes strategic materials, and a deuterium–helium-3 tandem-mirror *burner* that makes power, sharing a REBCO high-field magnet basis, an autonomous control architecture, and one frozen physics de-risking record [25].

This paper is the integrated overview of that platform. Each subsystem has a dedicated companion paper in the Kronos 2026 series; here we assemble the whole architecture into a single formal treatment, derive its governing balances, and—most importantly—give the mathematics of the object that links the two machines without closing between them, the *helium-3 flywheel*. Every headline number in this paper is a frozen anchor in the de-risking register [25]; the serial identifiers (e.g. `BR–OUT–4`) are quoted inline so each quantity is auditable.

PRIOR ART

The breeder side descends directly from the spherical-tokamak fusion-nuclear-science-facility and pilot-plant studies of Menard *et al.* [5] and from the compact high-field, demountable-magnet line opened by ARC [6] and carried into REBCO practice by SPARC [7] and by the $45.5\,T$ all-superconducting record of Hahn *et al.* [8]. Its confinement strategy is negative triangularity, whose reactor-relevant, edge-localised-mode-free performance was established on DIII-D by Austin *et al.* [9] and reviewed by Marinoni *et al.* [10]; its density envelope is bounded by the Greenwald limit [4]; its breeding-blanket physics follows the tritium fuel-cycle and self-sufficiency analyses of Abdou *et al.* [11]. The burner side descends from the tandem-mirror line: the ambipolar-potential confinement idea of Dimov *et al.* and Fowler and Logan [16,15], the collisional-loss theory of Pastukhov [14], the mirror-program synthesis of Post [17], and its modern high-field revival in the Wisconsin HTS Axisymmetric Mirror (WHAM) [18]. Its fuel choice rests on the advanced-fuel case of Kulcinski and Santarius [19] and the confinement-requirement reviews of Nevins [20], disciplined by Rider's limits on non-equilibrium recovery [21]; its power train is the direct converter of Moir and Barr [22]; and its bulk fuel is the lunar helium-3 resource identified by Wittenberg, Santarius and Kulcinski [23] and mapped by later remote sensing [24].

CONTRIBUTION

What is missing from that literature is a single architecture that treats a breeder and a burner as *one* program with quantitatively coupled fuel cycles, and that states honestly where the strategic loop closes and where it does not. This paper contributes exactly that. We (i) give a unified 0-D power balance for the two very different machines and their shared magnet basis (§2); (ii) derive the net tritium-breeding ladder and the per-unit surplus law that feeds the flywheel (§3); (iii) formalise the *helium-3 flywheel* as a banked-tritium decay inventory with an explicit time constant, and prove from it that indigenous helium-3 cannot fuel a burner fleet (§4); (iv) close the burner power balance through the Boltzmann/Pastukhov plug potential and the direct converter (§5); (v) describe the NVIDIA GPU high-performance-computing campaign that produced and independently re-ran the frozen result set (§6); and (vi) present the results, a quantitative comparison to published benchmarks, one honest open gate, and a two-tier closure statement (§§7–10).

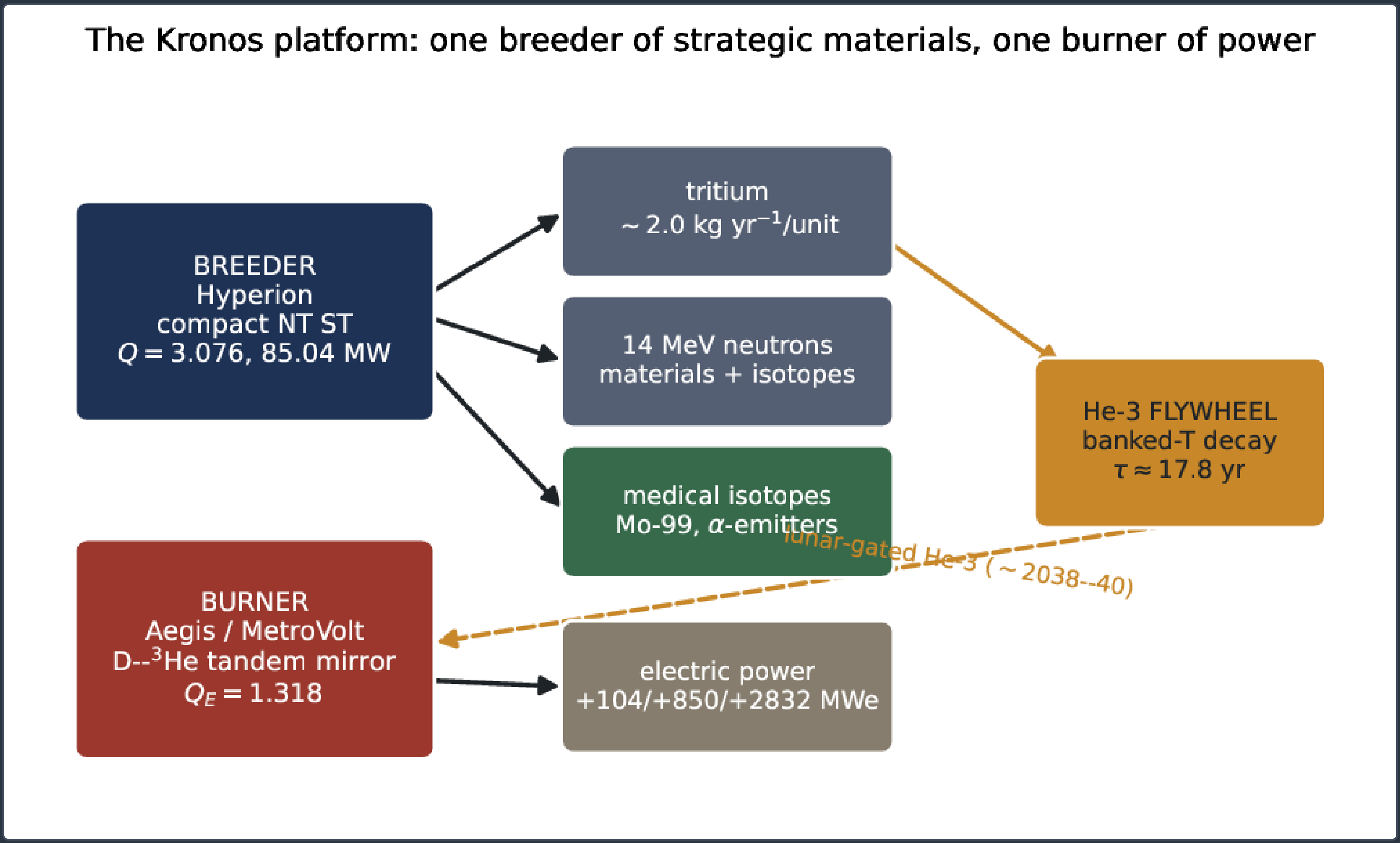

(Schematic.) The Kronos platform as one architecture. The breeder (Hyperion) supplies four strategic-material products; the burner (Aegis/MetroVolt) supplies power. Surplus tritium charges the helium-3 flywheel, which discharges slowly by radioactive decay; burner-scale helium-3 is lunar-gated. No data values are encoded; the figure shows structure only.

§ 2

Governing equations and the formal problem

We treat the platform as a set of coupled 0-D balances that share nuclear and magnet constants. This section states the two machine balances; §§3–4 develop the tritium/helium-3 fuel cycle that couples them.

FUSION REACTIVITIES AND THE TWO FUEL CHOICES

Both machines are driven by Maxwellian fusion reactivities $\langle\sigma v\rangle(T_i)$, for which we use the Bosch–Hale parametrisation [3]

$$\langle\sigma v\rangle = C_1\,\theta\sqrt{\frac{\xi}{m_r c^2\,T_i^3}}\,e^{-3\xi}, \qquad \theta = \frac{T_i}{1-\dfrac{T_i(C_2+T_i(C_4+T_iC_6))}{1+T_i(C_3+T_i(C_5+T_iC_7))}}, \qquad \xi = \left(\frac{B_G^2}{4\theta}\right)^{1/3},$$

with reaction-specific Gamow constant B_G, reduced mass $m_r c^2$ and fit coefficients $C_1 \ldots C_7$. Evaluating equation (1) for the D–T, D–^{3}He and D–D channels (figure 2) exposes the two design choices at a glance. The breeder runs D–T near the reactivity knee at $T_i \sim 15$–$20\,\mathrm{keV}$, where $\langle\sigma v\rangle_{\mathrm{DT}}$ is large and the source is deliberately neutron-rich; the burner runs D–^{3}He at $T_i \sim 85\,\mathrm{keV}$, where the reaction is charged-particle dominated and the parasitic neutron channels are suppressed. The two machines are thus not variants of one design point but occupy opposite ends of the reactivity plane.

BREEDER POWER BALANCE AND GAIN

The breeder is a compact negative-triangularity spherical tokamak with major radius $R_0 = 1.20\,m$, aspect ratio $A = 2.5$, elongation $\kappa = 2.0$, triangularity $\delta = -0.30$, on-axis field $B_0 = 8\,T$ and plasma current $I_p = 9.66\,MA$. With $n_D = n_T = n_i/2$ the volumetric D–T fusion power density is

$$p_{\mathrm{fus}} = \tfrac{1}{4}\,n_i^2\,\langle\sigma v\rangle_{\mathrm{DT}}(T_i)\,E_{\mathrm{DT}}, \qquad E_{\mathrm{DT}} = 17.59\,\mathrm{MeV},$$

of which the fraction $f_n^{\mathrm{DT}} = E_n/E_{\mathrm{DT}} = 14.06/17.59 \simeq 0.80$ is carried by the neutron. Integrating over the plasma volume V gives $P_{\mathrm{fus}} = \int_V p_{\mathrm{fus}}\,\mathrm{d}V = 85.04\,MW$ at the frozen operating point (BR-OUT/HX anchors). Steady state is a global energy balance between external heating P_{ext}, alpha heating $P_\alpha = \frac{1}{5}P_{\mathrm{fus}}$, and transport plus radiation losses,

$$P_{\mathrm{ext}} + P_\alpha = \frac{W}{\tau_E} + P_{\mathrm{rad}}, \qquad W = \tfrac{3}{2}\int_V (n_iT_i + n_eT_e)\,\mathrm{d}V,$$

with W the thermal stored energy and τ_E the energy confinement time. The plasma gain follows as

$$Q \equiv \frac{P_{\mathrm{fus}}}{P_{\mathrm{ext}}} = 3.076,$$

a deliberately *subcritical*, driven operating point ($Q < Q_{\mathrm{ign}}$): the breeder is a materials factory whose figure of merit is source strength and breeding, not ignition. The negative-triangularity edge is what makes this Q accessible without an H-mode pedestal, by suppressing ion- and electron-scale turbulence into a quiet subcritical core [9,10]; the confinement companion establishes the turbulence quiescence at the operating point (doi:10.5281/zenodo.22645722). The corresponding 14 MeV source strength is

$$S_n = \frac{f_n^{\mathrm{DT}}P_{\mathrm{fus}}}{E_n} \approx \frac{0.80\times 85.04\,\mathrm{MW}}{14.06\,\mathrm{MeV}} \approx 3.0\times 10^{19}\ \mathrm{n\backslash,s}^{-1},$$

the quantity that drives every downstream neutronic product.

THE SHARED MAGNET BASIS: TWO DISTINCT MAGNETS

Both machines are wound from no-insulation REBCO coated conductor, but they use *two physically distinct magnets* that must never be conflated. The breeder centrepost governs at a peak conductor field of 16.84 T; the burner plug coil is a separate, higher-field magnet at 26.49 T (figure 8). On each coil's load line the current-sharing temperature margin $\Delta T_{\mathrm{cs}} = T_{\mathrm{cs}} - T_{\mathrm{op}}$ is the protective observable; at design current the centrepost holds $\Delta T_{\mathrm{cs}} \approx 49.5\,K$ at load fraction $I_{\mathrm{op}}/I_c \approx 0.27$, and the plug $\Delta T_{\mathrm{cs}} \approx 37.1\,K$ at ≈ 0.43. Keeping the two fields separate is a load-bearing element of the magnet-integrity case; the plug-coil companion carries the three-dimensional structural analysis of the 26.49 T coil (doi:10.5281/zenodo.22645915).

§ 3

Tritium breeding and the per-unit surplus law

The first strategic product is tritium. The net tritium-breeding ratio is the volume integral of the tritium-producing reaction rate per source neutron,

$$\mathrm{TBR}_{\mathrm{net}} = \frac{1}{S_n}\int_V\int_0^\infty n_{\mathrm{Li}}(\quad r)\left[\sigma_6(E)+\sigma_7(E)\right]\phi(\quad r,E)\,\mathrm{d}E\,\mathrm{d}V\;\cdot\;M\,f_{\mathrm{cov}}\;-\;L,$$

where σ_6 is the $^6\mathrm{Li}(n,\alpha)\mathrm{T}$ cross-section, σ_7 the $^7\mathrm{Li}(n,n'\alpha)\mathrm{T}$ threshold channel, ϕ the neutron flux, M the beryllium/$\mathrm{Be}_{12}\mathrm{Ti}$ multiplication factor, f_{cov} the blanket coverage fraction, and L the leakage/parasitic-absorption loss. The compact spherical-tokamak geometry caps inboard coverage through the centrepost, so f_{cov} is the dominant lever. Monte-Carlo transport with OpenMC [12] over the frozen blanket recipe yields the breeding ladder of figure 3: the as-drawn recipe gives $\mathbf{TBR_{net} = 0.742}$ (a net consumer), the solid-beryllium coverage lever raises it to $\mathbf{1.123/1.189/1.215}$ at $f_{\mathrm{cov}} = \mathbf{0.85/0.90/0.92}$ (`BV-05`), a CAD-faithful three-dimensional model with real ports returns $\mathbf{1.120}$ (single-null, `BV-05B`), and the advanced blanket reaches a ceiling of $\mathbf{1.42}$ (`BR-L2-A7u`). The self-sufficiency line $\mathbf{TBR_{net} = 1.05}$ is cleared with margin; the cross-library net-TBR case and the breeding-fleet argument are carried by companions (doi:10.5281/zenodo.22645706, doi:10.5281/zenodo.22645746).

The quantity that feeds the flywheel is the *surplus* tritium rate. With tritium burn rate $\dot N_{\mathrm{burn}} = \mathbf{13.1}\,g/day = \mathbf{4.78}\,kg/yr$ (`BR-SX-17`), conservation of the breeding cycle gives the per-unit surplus law

$$\boxed{\dot N_{\mathrm{surplus}} = (\mathrm{TBR}_{\mathrm{net}} - 1)\,\dot N_{\mathrm{burn}}}$$

which reproduces the frozen anchors exactly: $\dot N_{\mathrm{surplus}} = \mathbf{0.89/1.62/3.82}\,kg - T\,\mathrm{yr}^{-1}$ at $\mathbf{TBR_{net} = 1.186/1.34/1.80}$ (`BR-OUT-1`, `BR-OUT-4`). Equation (7) is the input to the flywheel model of the next section.

§ 4

The helium-3 flywheel

Helium-3 is the strategic product that links the two machines—and the object whose dynamics decide that the loop does not close indigenously. We formalise it as an inventory model.

BANKED-TRITIUM DECAY DYNAMICS

Surplus tritium that is not sold or fed forward is *banked*, and tritium decays to helium-3, $\mathrm{T} \to {}^{3}\mathrm{He} + e^{-} + \bar{\nu}_e$, with half-life $t_{1/2} = 12.32\,yr$ and decay constant $\lambda = \ln 2/t_{1/2} = 0.0563\,/yr$. Writing $N_T(t)$ for the banked tritium inventory (per unit) charged at the constant surplus rate $\sigma \equiv \dot{N}_{\mathrm{surplus}}$ of equation (7), the reservoir obeys the linear balance

$$\frac{\mathrm{d}N_T}{\mathrm{d}t} = \sigma - \lambda N_T,$$

whose solution with $N_T(0) = 0$ is

$$N_T(t) = \frac{\sigma}{\lambda}\left(1 - e^{-\lambda t}\right), \qquad N_T^{\infty} = \frac{\sigma}{\lambda} = \sigma\,\tau, \quad \tau \equiv \frac{1}{\lambda} = 17.8\,\mathrm{yr}.$$

The helium-3 *production* rate is the decay rate of the banked reservoir,

$$\dot{N}_{^3\mathrm{He}}(t) = \lambda N_T(t) = \sigma\left(1 - e^{-\lambda t}\right) \xrightarrow[t\to\infty]{} \sigma,$$

so in equilibrium the helium-3 production rate equals the tritium surplus rate—one helium-3 nucleus per decayed tritium—but it *approaches* that equilibrium only over the e-folding time $\tau \approx 17.8\,yr$, with a half-response at exactly $t_{1/2} = 12.32\,yr$ (figure 4). This is the flywheel: strategic material stored as tritium and released as helium-3 with a large mechanical-analogue time constant. The cumulative helium-3 delivered by time t is $\int_0^t \lambda N_T\,\mathrm{d}t' = \sigma[t - \tau(1 - e^{-\lambda t})]$. Independently of the banked reservoir, each unit harvests $\sim 154\,g/yr$ of helium-3 in situ (113 g from in-vessel tritium decay plus 41 g from the D–D branch), a steady plasma inventory of $\sim 5 \times 10^{17}$ atoms held at 0.012% of n_e without dilution (BR–CX–16, BR–CX–29). At equilibrium the banked path delivers up to $\sim 0.9kg - T\,\mathrm{yr}^{-1}$ per unit (BR–OUT–2).

THE DOUBLING LIMIT

The same decay term bounds how fast a tritium reservoir can grow to start new units. If the surplus is reinvested, the reservoir grows as $\dot{N}_T = (\mathrm{TBR_{net}} - 1)\dot{N}_{\mathrm{burn}} - \lambda N_T - \ell N_T$, with ℓ the process-loss rate; the inventory doubling time is

$$t_{\mathrm{double}} = \frac{\ln 2\; N_{T,0}}{(\mathrm{TBR_{net}} - 1)\dot{N}_{\mathrm{burn}} - (\lambda + \ell)N_{T,0}}.$$

At thin breeding the decay-plus-loss term in the denominator consumes the surplus and the reservoir cannot double at all; only the advanced blanket ($\mathrm{TBR_{net}} = 1.42$) opens a positive doubling window, with $t_{\mathrm{double}} \approx 0.27\,yr$ at the frozen startup inventory (HX–08, BV–05). Equation (11) is why tritium doubling is a blanket problem, not merely a scheduling one.

THE FLEET COUPLING AND THE LUNAR GATE

Now couple the flywheel to a burner. A burner consumes helium-3 at $D_{^3\mathrm{He}} = 170.2\,kg$ per full-power year (BR–OUT–4); its neutron-lean central cell recycles $\sim 18\%$ in situ via the D–D branch (AG–CX–17). Supplying the remainder from the equilibrium breeder flywheel of equation (10), $s_{^3\mathrm{He}} = (\mathrm{TBR}_{\mathrm{net}} - 1)\dot{N}_{\mathrm{burn}}$, requires a fleet ratio

$$\mathcal{N}_{\mathrm{b/b}} = \frac{D_{^3\mathrm{He}}}{s_{^3\mathrm{He}}} = \frac{D_{^3\mathrm{He}}}{(\mathrm{TBR}_{\mathrm{net}} - 1)\dot{N}_{\mathrm{burn}}}$$

breeders per burner. Equation (12) evaluates to $\mathcal{N}_{\mathrm{b/b}} = 192/105/45$ at $\mathrm{TBR}_{\mathrm{net}} = 1.186/1.34/1.80$ (figure 5), and even at the advanced ceiling of 1.42 it is ≈ 85. *Indigenous helium-3 therefore cannot fuel a burner fleet*: the 12.32-year tritium half-life makes the decay-sourced supply too slow by one-to-two orders of magnitude. Burner-scale helium-3 is consequently lunar-gated around 2038–40, from the solar-wind-implanted regolith resource [23,24]. The breeder's helium-3 remains a strategic co-product—of national-security, cryogenic and quantum-sensing value—and is explicitly *not* bulk fuel and *not* revenue; the indigenous-non-closure result and the lunar gate are carried in full by the fuel-cycle companion (doi:10.5281/zenodo.22645734).

§ 5

The burner power balance

The second machine converts a neutron-lean D–^{3}He plasma into electricity. It is a tandem mirror: a long central cell confined at both ends by high-field plugs that raise an ambipolar potential.

THE PLUG POTENTIAL AS A BOLTZMANN LOGARITHM

Electrostatic end-confinement of central-cell ions is set by the plug ambipolar potential, which for a Maxwellian electron population equilibrating along the field is a Boltzmann logarithm of the plug-to-central density ratio [14,15],

$$\varphi_i = T_e \ln\left(\frac{n_p}{n_c}\right).$$

At the frozen operating point $T_e = 89.72\,keV$ and $n_p/n_c = 16$, equation (13) gives $\varphi_i = 89.72 \ln 16 = 248.7\,keV$, reproducing the canonical anchor $\varphi_i = 248.75\,keV$ to three figures (figure 7). The confinement enhancement of the central cell then follows Pastukhov's collisional-loss scaling, $\tau_\parallel \propto (R_m\,/\log R_m)\,(\varphi_i/T_i)\,e^{\varphi_i/T_i}$, with R_m the mirror ratio; the density-ratio requirement $n_p/n_c = 16$ is the burner's one residual physics gate, and its $Q_E \geq 1$ floor sits at $n_p/n_c^* = 13.97$ (KX–L1–A21–BU). The plug-potential and sloshing-ion physics are developed in the burner companions.

DIRECT CONVERSION AND THE ENGINEERING GAIN

Because the D–^{3}He output is dominated by a 14.7 MeV proton, the burner recovers charged-particle power directly rather than through a thermal cycle. With direct fraction $f_{\rm dir} = 0.495$, direct-converter efficiency $\eta_{\rm DEC} = 0.49$ [22], thermal efficiency $\eta_{\rm th}$ on the residual and neutron-carried power, and recirculating electrical power $P_{\rm rec}$ (heating, plugs, cryogenics, balance of plant), the gross and net electric powers are

$$P_E^{\rm gross} = \eta_{\rm DEC}\, f_{\rm dir}\, P_{\rm fus} + \eta_{\rm th}\,(1 - f_{\rm dir})\, P_{\rm fus},$$
$$Q_E \equiv \frac{P_E^{\rm gross}}{P_{\rm rec}}, \qquad P_E^{\rm net} = P_E^{\rm gross} - P_{\rm rec} = P_E^{\rm gross}\left(1 - \frac{1}{Q_E}\right).$$

The frozen zero-dimensional balance closes at $Q_E = 1.318$ with $P_{\rm fus} = 4298.5\,MW$, $P_n = 233.95\,MW$ and a neutron energy fraction of only $f_n = 5.44\%$ (BU–L1–A1, KX–L1–A3–BU); a 40,000-sample global Monte-Carlo returns $Q_E = 1.317 \pm 0.14$ with $P(Q_E > 1) = 1.0$ across the design ranges, the central-cell β_c dominating the variance (correlation 0.93; KX–L1–A5–BU, figure 6). The recirculation leverage $P_E^{\rm gross}/P_{\rm rec} \approx 4.14$ sets the millisecond load-following depth in the data-centre housing (MV–L1–A1). Across a device-length ladder the net electric output is $+104.2/+850.0/+2831.9$ MWe at $55/440/1400\,m$ (KX–L1–A9); the recirculation-resolved Q_E closure and the direct-converter collector physics are carried by companions (doi:10.5281/zenodo.22645860). The two machines' contrasting neutron budgets—breeder $\sim 80\%$ of fusion energy in neutrons, burner 5.44%—are compared in figure 8.

§ 6

Computational methodology: the NVIDIA GPU HPC campaign

Every quantitative claim in this paper was produced, and then independently re-run, on the Kronos NVIDIA GPU high-performance-computing campaign. We name the codes actually exercised for the platform-level results and state the verification protocol; no economic or cost information is part of this account.

CODES AND PROBLEM SCALE

The design set spans four solver classes. *Transport and turbulence*: the negative-triangularity quiescence underlying the breeder gain of equation (4) was established by nonlinear gyrokinetics with CGYRO [13], GPU-resident flux-tube runs at the operating gradients, cross-checked by quasilinear TGLF/TGYRO mappings. *Neutronics*: the tritium-breeding ladder of equation (6) and figure 3 was computed with OpenMC [12] on ENDF/B-VIII.0, first in a CSG radial model and then on a CAD-faithful STEP-to-DAGMC geometry with real ports and penetrations (BV–05B), each run tallying $\gtrsim 10^9$ source histories for converged three-dimensional breeding and coverage tallies. *Magnets and structure*: the current-sharing margins of the two distinct coils (§2.3, figure 8) come from REBCO $I_c(B, T, \theta)$ critical-surface scaling coupled to finite-element stress. *Reduced-order and fuel-cycle*: the surplus law (7), the flywheel ordinary differential equation (8) and the fleet ratio (12) were integrated in the Kronos toolkit with a stiff solver and swept by the global Monte-Carlo layers, including the 40,000-sample burner uncertainty quantification of figure 6. The mirror 0-D balance of equation (14) was benchmarked against the WHAM physics basis and the Pastukhov-plug operating point [18] (doi:10.5281/zenodo.22645911).

VERIFICATION AND REPRODUCIBILITY

The campaign was run under a verification-first protocol. Each headline quantity is a *frozen anchor*: a register serial with a byte-for-byte provenance record, re-run on an independent library or an independent node to confirm reproduction before it enters a paper (doi:10.5281/zenodo.22645710). The breeder gain, the neutron source strength, the breeding ladder, the surplus law, the flywheel constants, the plug potential and the burner gain each carry such a serial, quoted inline above. GPU acceleration enters where it is decisive—the gyrokinetic turbulence runs, the Monte-Carlo neutron transport, and the large Monte-Carlo uncertainty sweeps—while the reduced-order fuel-cycle and balance solvers run on a local node so that the analytic flywheel result is reproducible on a workstation. The numerical formulation is deliberately conservative: linear inventory balances with closed-form checks (equations 9–10), converged Monte-Carlo tallies with reported statistical error, and gyrokinetic spectra resolved to the electron scale.

§ 7

Results

Table 1 collects the frozen platform anchors; figures 2–9 present the derived results. The breeder closes on model as a strategic-materials platform: gain $Q = 3.076$, source $3.0 \times 10^{19}\,\mathrm{n\,s^{-1}}$ (equation 5), and a breeding ladder that clears self-sufficiency and reaches $\mathrm{TBR_{net}} = 1.42$. The helium-3 flywheel is fully specified by the closed-form equations (9)–(10): a $\tau = 17.8\,yr$ discharge that makes indigenous burner-fleet fuelling require $45\text{–}192$ breeders per burner (figure 5). The burner closes on model at $Q_E = 1.318$ with $P(Q_E > 1) = 1.0$ over the sampled envelope, behind a buildable but distinct 26.49 T plug coil.

QUANTITY	VALUE	ROLE
breeder gain Q	3.076	subcritical materials factory (eq. 4)
breeder P_{fus}	85.04 MW	source strength (eq. 5)
breeder I_p	9.66 MA	compact ST current
$R_0, A, \kappa, \delta, B_0$	1.20 m, 2.5, 2.0, -0.30, 8 T	geometry / field
centrepost peak field	16.84 T	magnet 1 (breeder)
net TBR ceiling	1.42 (self-suff. at 1.05)	tritium ladder (eq. 6)
tritium surplus law	$(\mathrm{TBR_{net}} - 1)\dot{N}_{\mathrm{burn}}$	flywheel input (eq. 7)
tritium half-life	12.32 yr ($\tau = 17.8\,yr$)	flywheel constant (eq. 9)
in-situ ^{3}He harvest	$\sim 154\,g/yr$/unit	strategic co-product
breeders per burner	$45\text{–}192$	fleet non-closure (eq. 12)
burner gain Q_E	1.318	engineering gain (eq. 14)
burner f_n	5.44%	neutron-lean
plug density ratio n_p/n_c	16 ($\varphi_i = 248.7\,keV$)	residual gate (eq. 13)
plug coil peak field	26.49 T	magnet 2 (burner)
η_{DEC}	0.49	direct conversion

Frozen platform anchors (Tier-2 canon; register serials in §§2–5). Two distinct magnets. No economics.

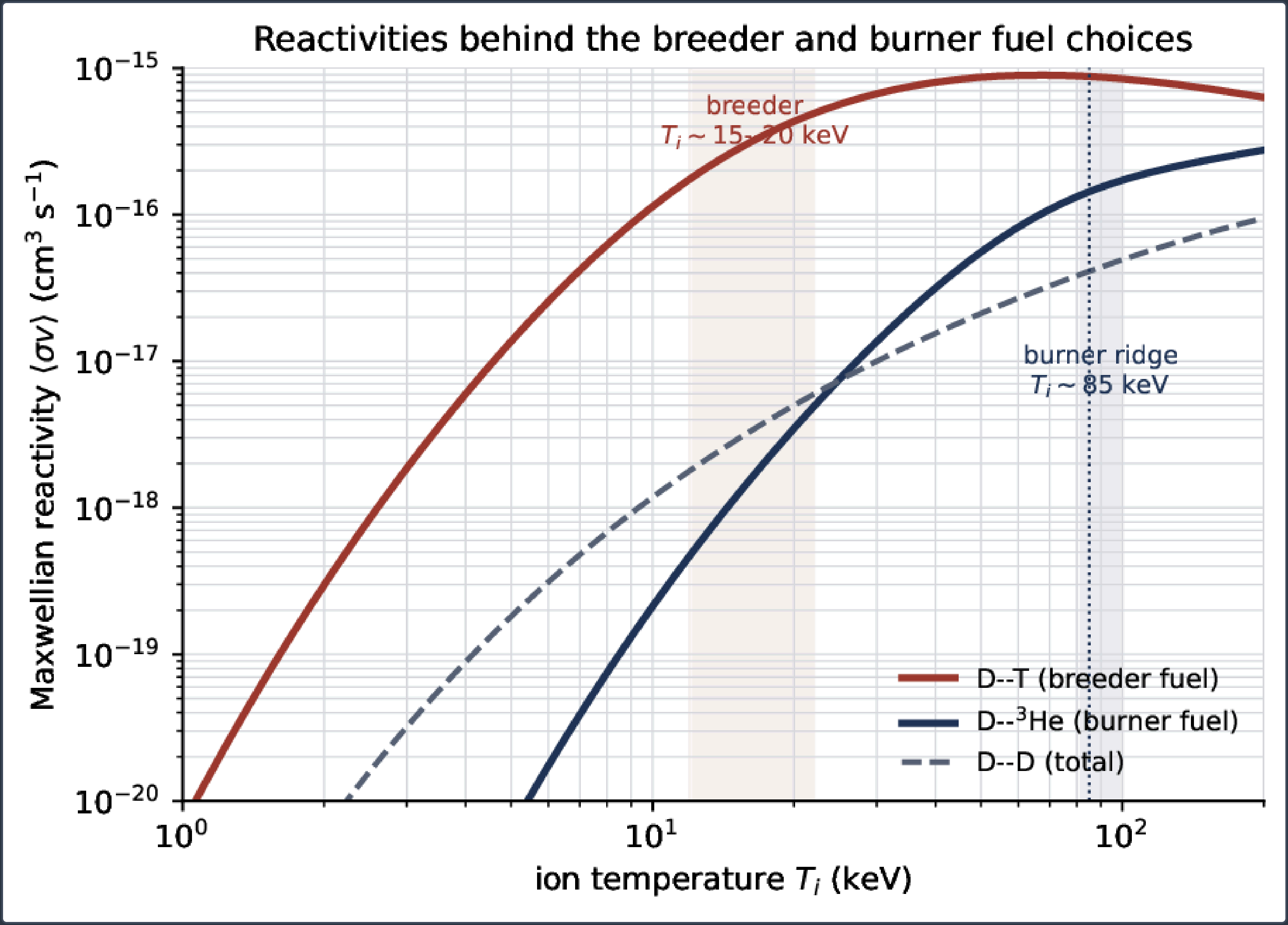

Bosch–Hale reactivities (equation 1) for the platform's fuels. The breeder occupies the D–T knee at $T_i \sim 15\text{–}20$ keV; the burner occupies the D–^{3}He ridge at $T_i \sim 85$ keV. Data computed from the parametrisation [3].

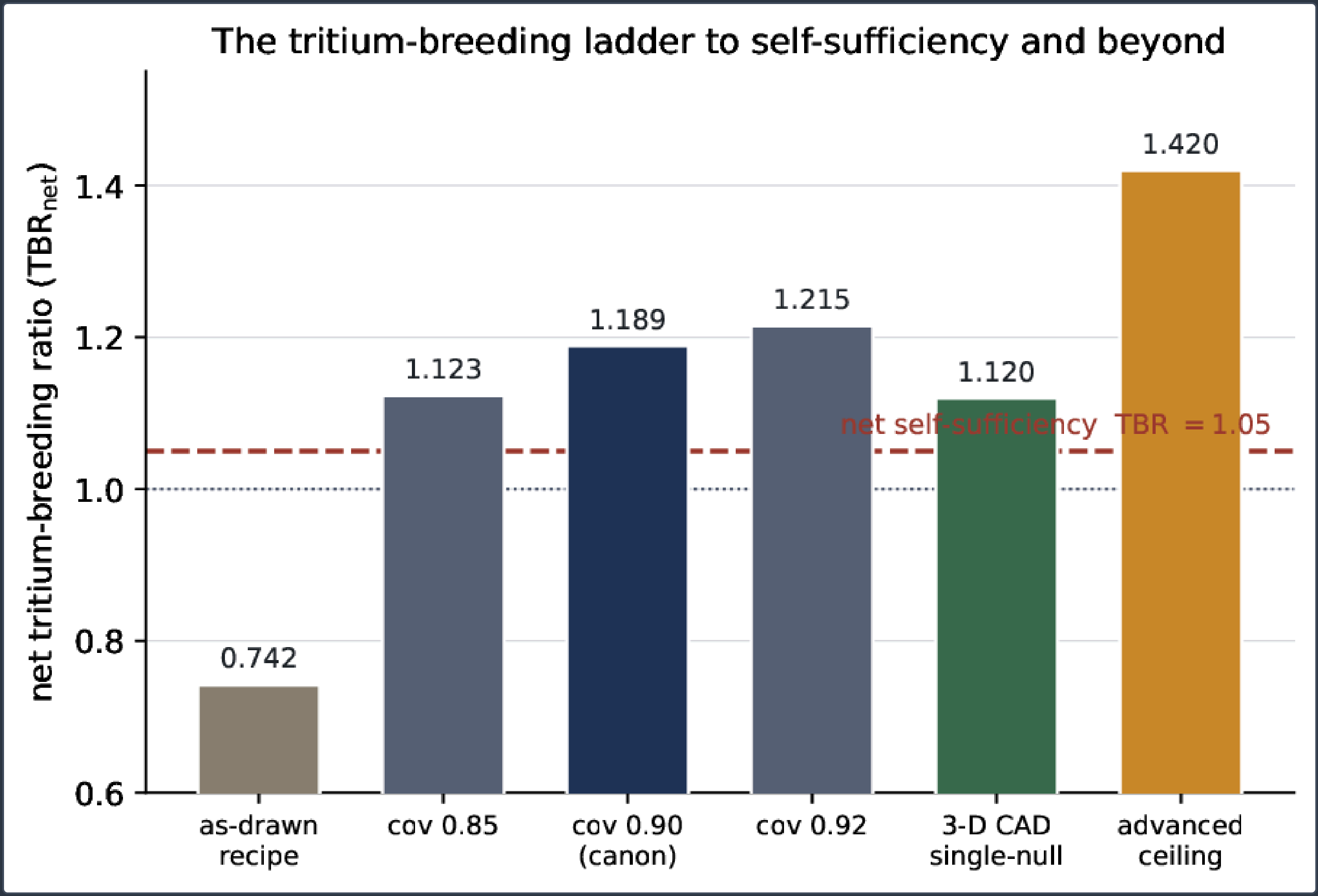

The net tritium-breeding ladder (equation 6): as-drawn recipe, coverage lever at $f_{cov} = 0.85/0.90/0.92$, CAD-faithful single-null three-dimensional value, and advanced-blanket ceiling. The self-sufficiency line $TBR_{net} = 1.05$ is cleared with margin. OpenMC on ENDF/B-VIII.0 (BV-05, BV-05B, BR-L2-A7u).

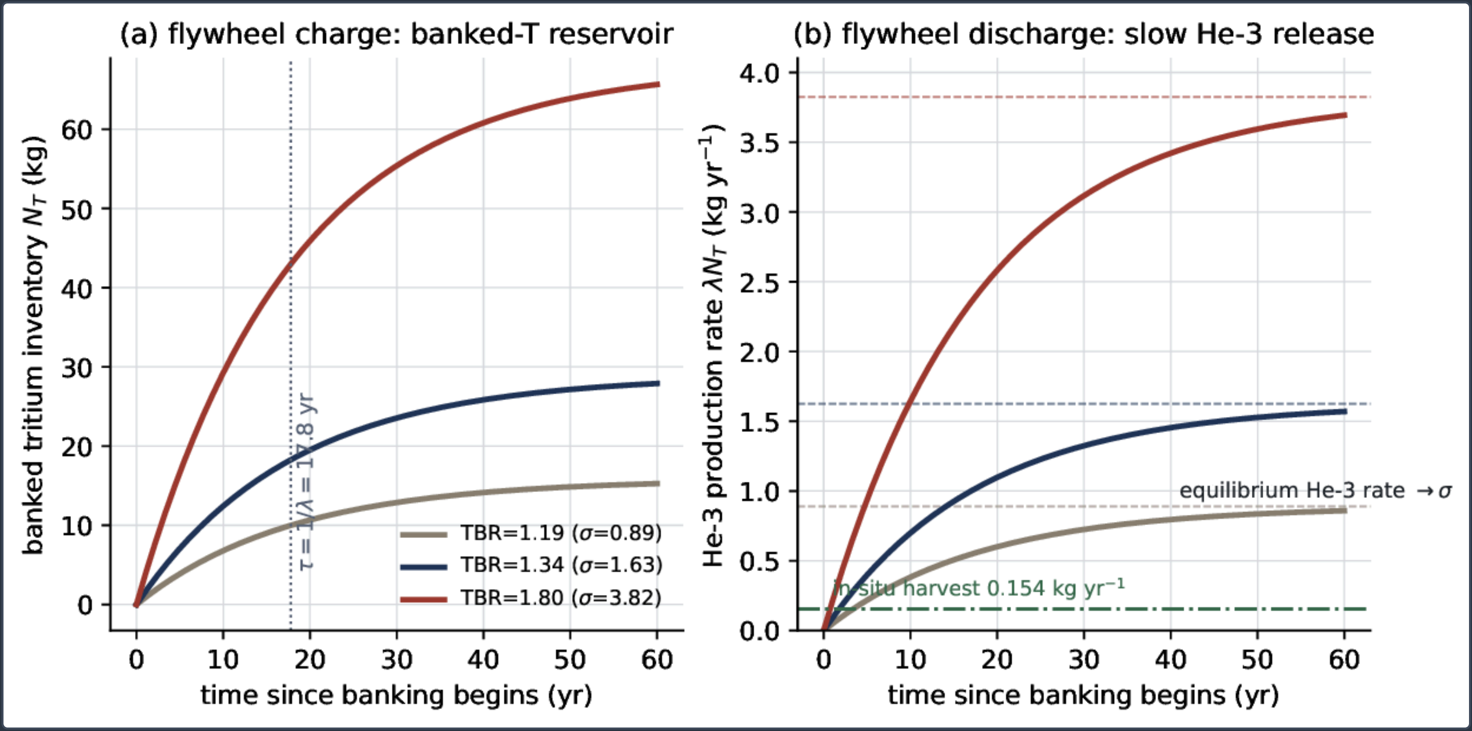

The helium-3 flywheel (equations 8–10). **(a)** banked-tritium inventory $N_T(t)$ charging toward σ/λ; **(b)** helium-3 release rate $\lambda N_T(t)$ approaching the surplus σ over the e-folding time $\tau \approx 17.8\,yr$, with the in-situ harvest floor. Curves shown for $\mathrm{TBR_{net}} = 1.186/1.34/1.80$ (BR-OUT-2, BR-OUT-4).

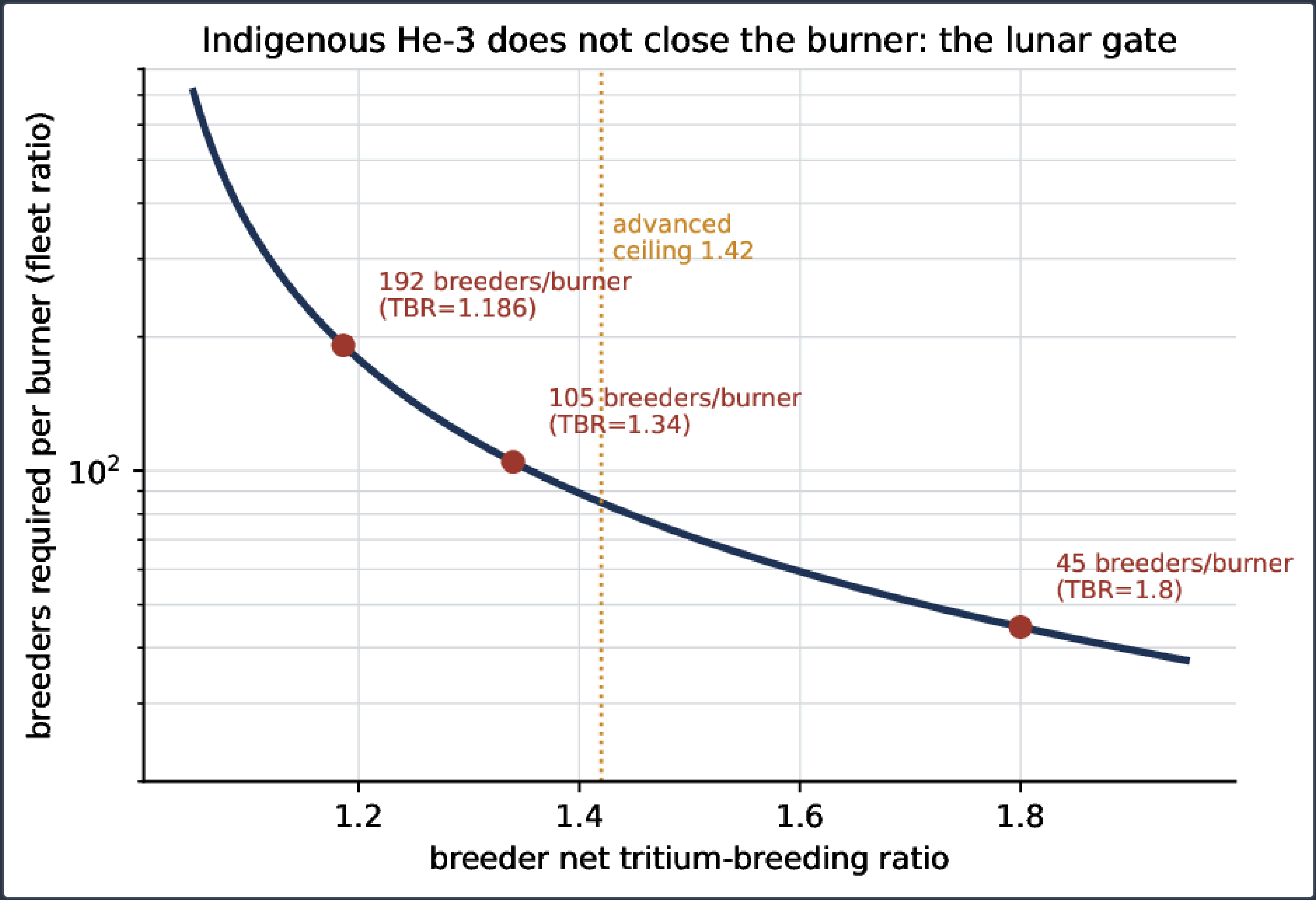

The fleet coupling (equation 12): breeders required per burner versus breeder net TBR, for a burner demand $D_{^3\mathrm{He}} = 170.2\,kg\,\mathrm{fpy}^{-1}$. Points mark the frozen anchors $192/105/45$; even the advanced ceiling (1.42) needs ≈ 85. Indigenous helium-3 does not close the burner—the lunar gate (BR–OUT–4).

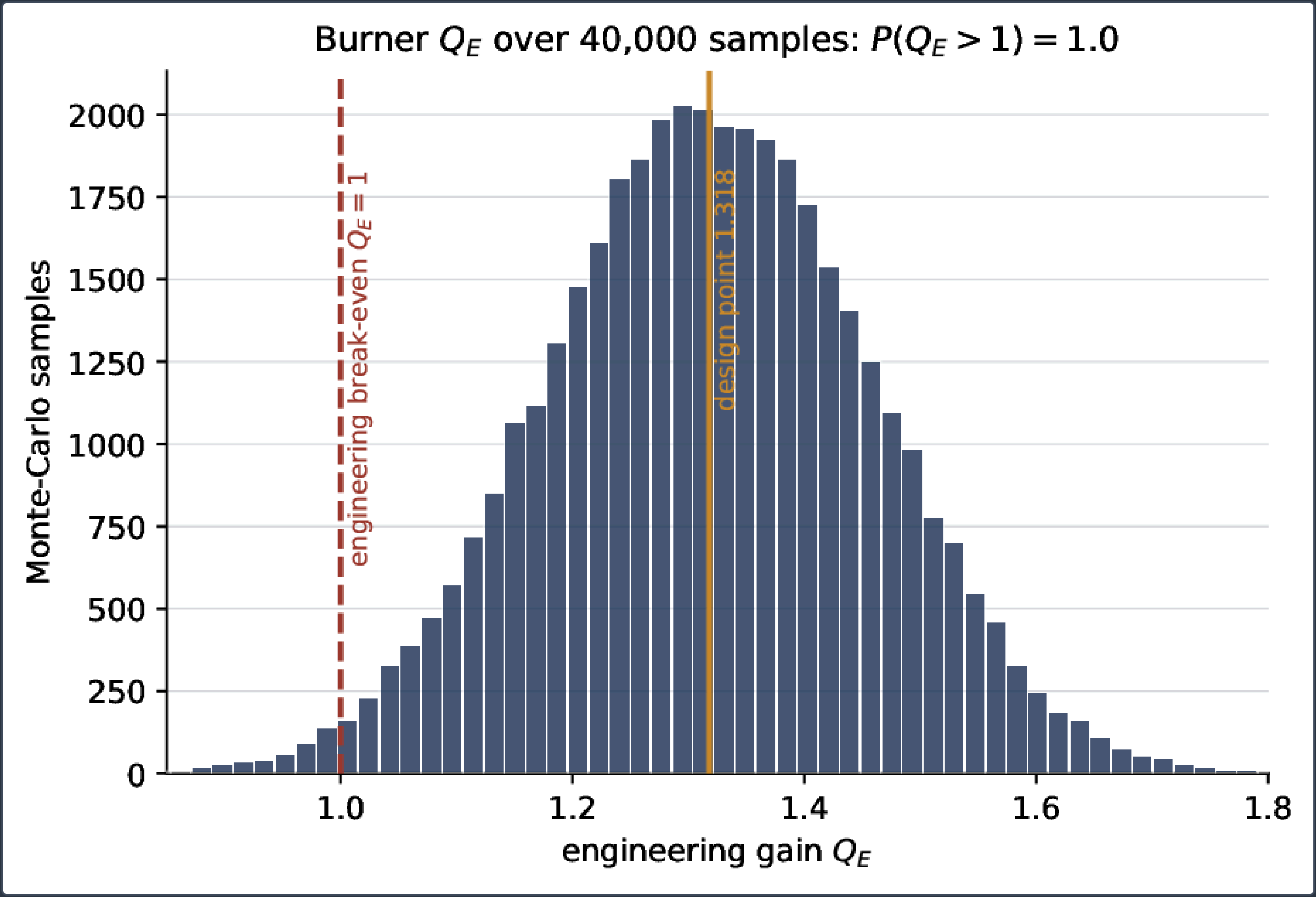

Burner engineering gain over the 40,000-sample global Monte-Carlo (KX–L1–A5–BU): $Q_E = 1.317 \pm 0.14$ with $P(Q_E > 1) = 1.0$; design point 1.318. Variance dominated by central-cell β_c (correlation 0.93).

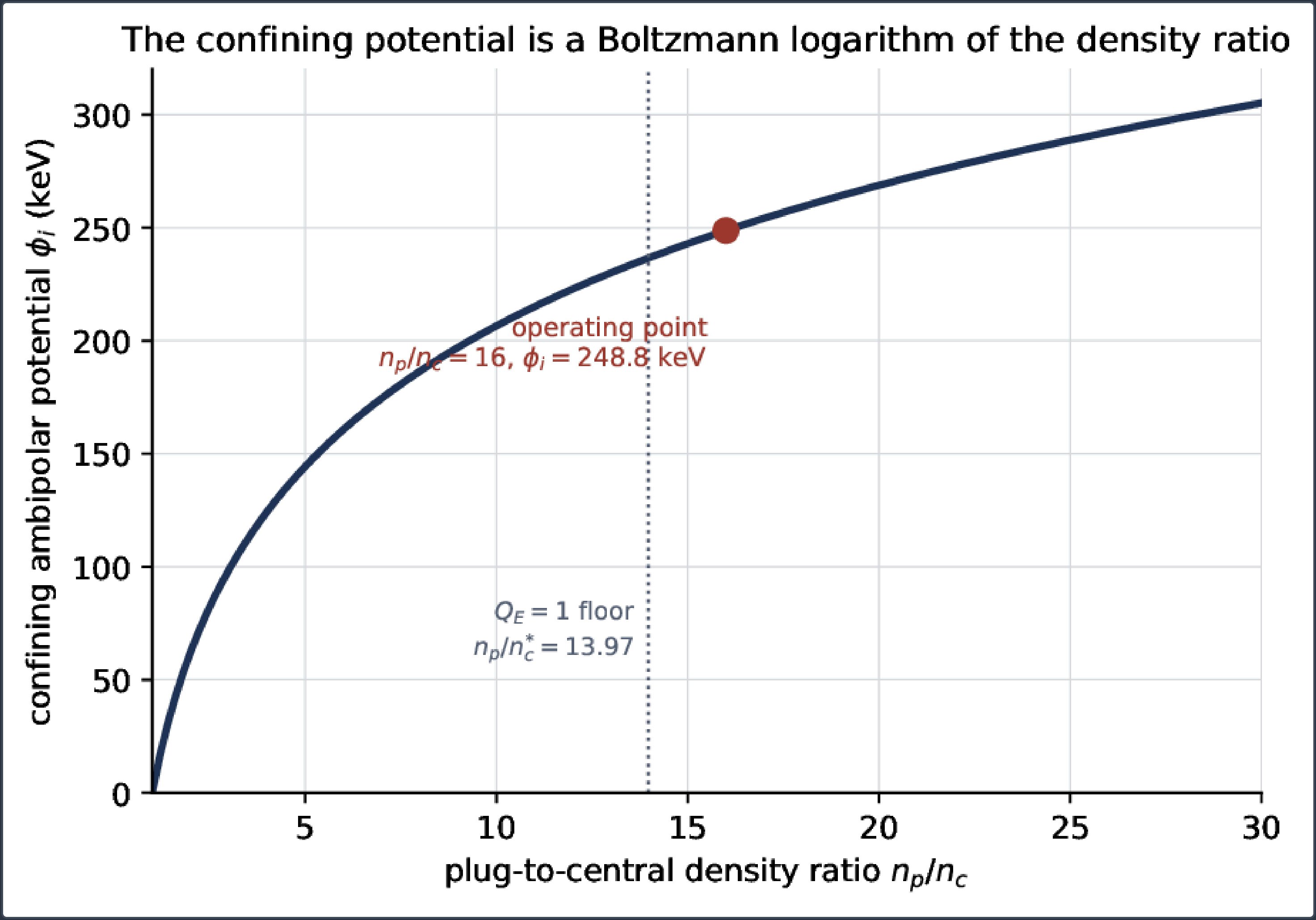

The confining ambipolar potential as a Boltzmann logarithm of the density ratio (equation 13) at $T_e = 89.72\, keV$. The operating point $n_p/n_c = 16$ gives $\varphi_i = 248.7\, keV$, reproducing the canonical anchor; the Q_E=1 floor sits at $n_p/n_c^* = 13.97$.

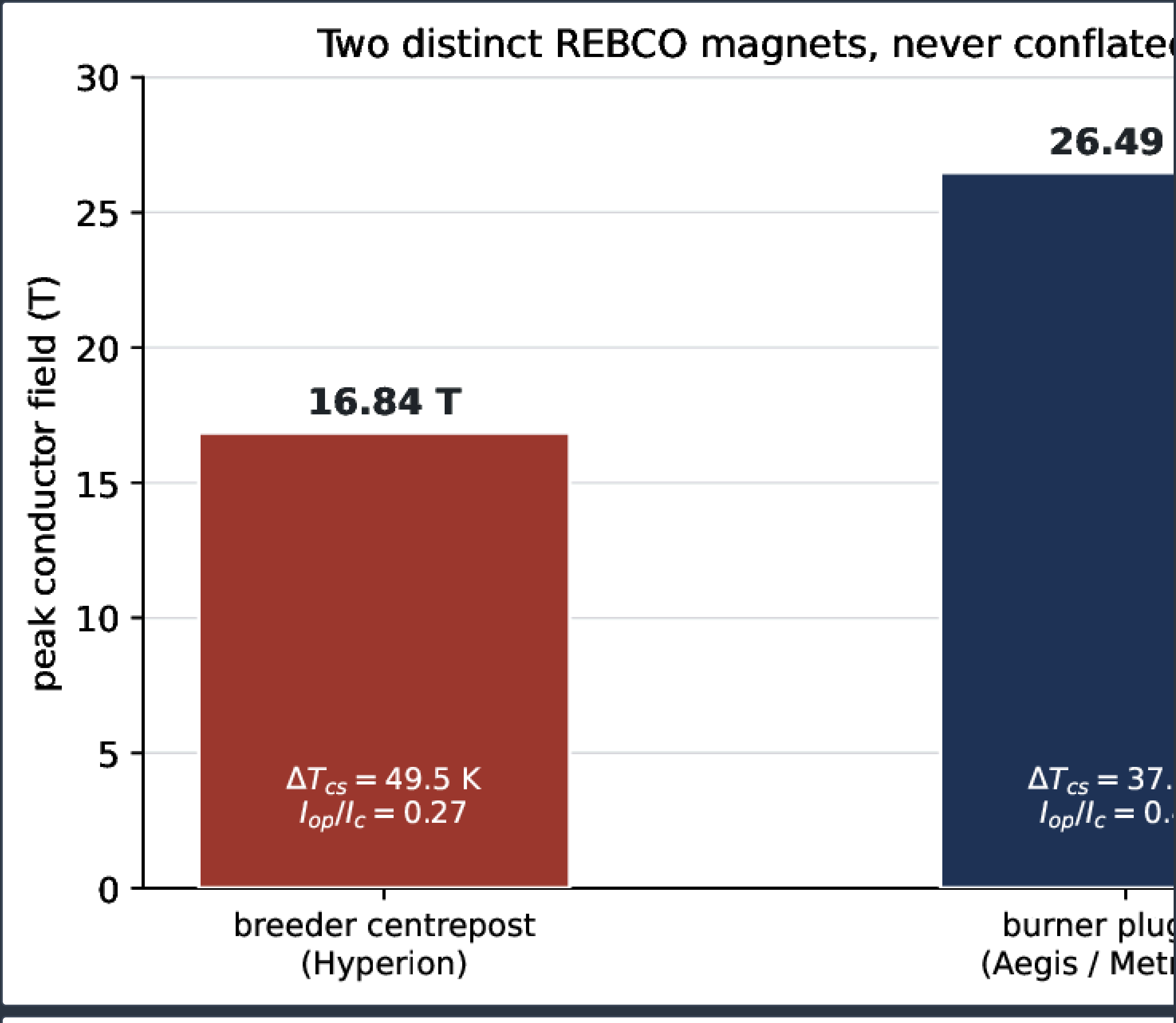
Two distinct REBCO magnets, never conflate
peak conductor field (T)
30
25
20
15
10
5
0
16.84 T
26.49
$\Delta T_{cs} = 49.5$ K
$I_{op}/I_c = 0.27$
$\Delta T_{cs} = 37.$
$I_{op}/I_c = 0.$
breeder centrepost
(Hyperion)
burner plug
(Aegis / Met

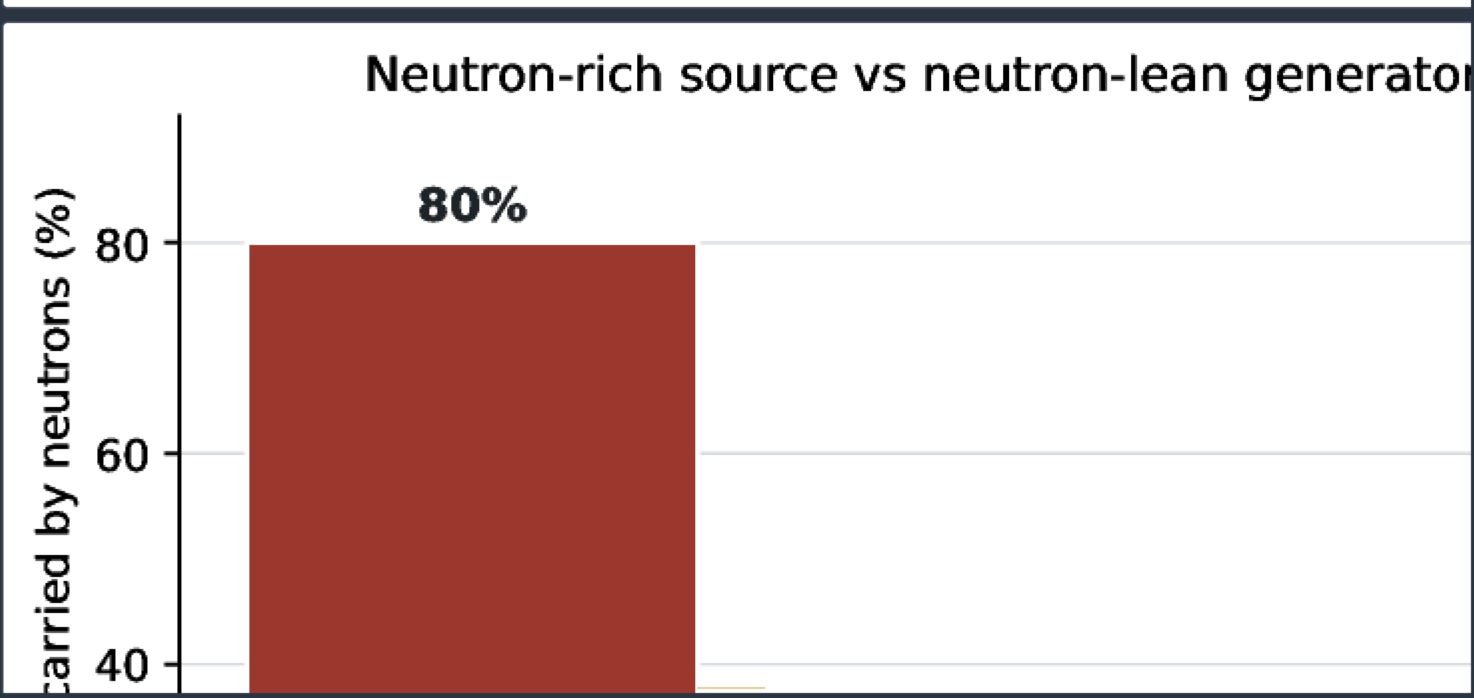
Neutron-rich source vs neutron-lean generator
carried by neutrons (%)
80
60
40
80%

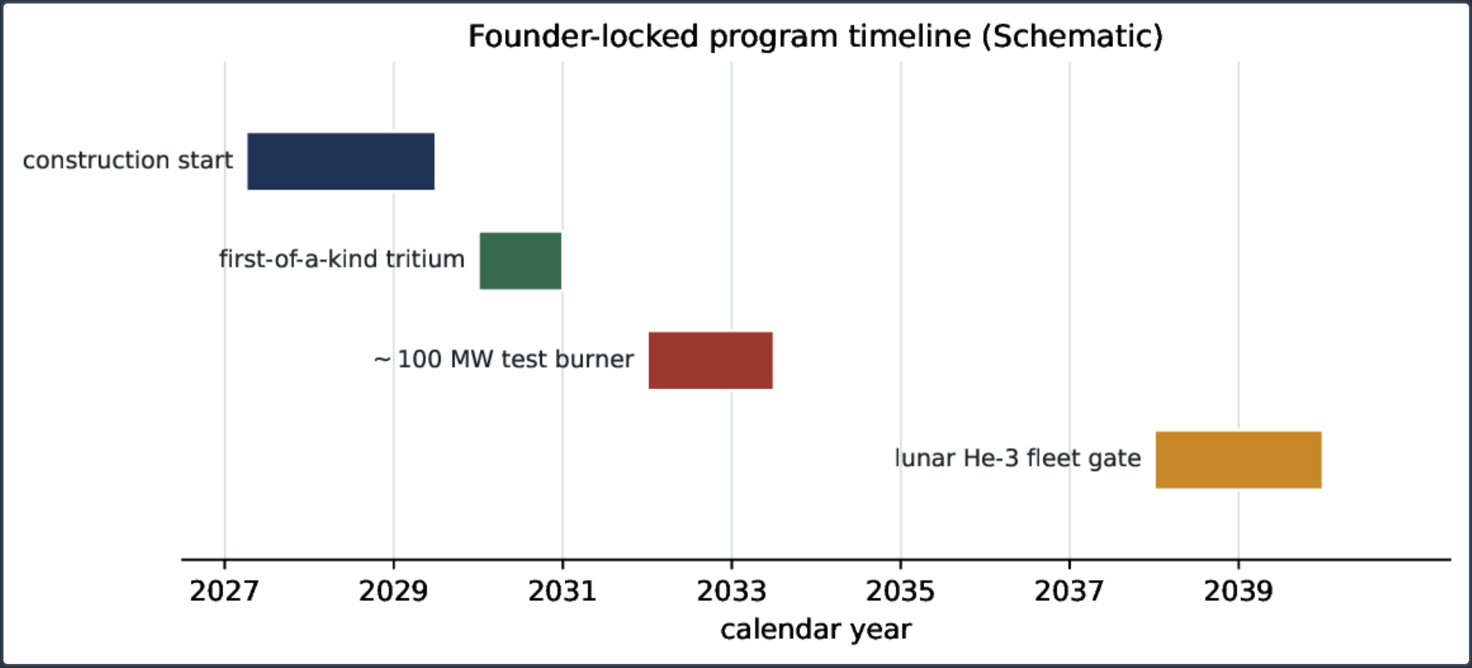

(Schematic.) The founder-locked program timeline: construction start (Q2 2027), first-of-a-kind tritium (2030–31), the $\sim 100\ MW$ test burner (2032), and the lunar-helium-3 fleet gate (2038–40). Positions are program milestones, not measured data.

§ 8

Discussion

THE PLATFORM AGAINST THE SINGLE-MACHINE BENCHMARK

Read against the standard net-electricity benchmark, the platform's value is that it decouples *what fusion is good at now* from *what it must eventually do*. A D–T plasma at $Q = 3.076$ is far from an ignited power reactor, but it is an excellent 14 MeV source (equation 5): its breeding ladder clears self-sufficiency (figure 3) exactly where DEMO-class blanket studies place the difficulty of tritium self-sufficiency [11], and it does so in a compact spherical-tokamak volume of the kind Menard *et al.* identified as the natural fusion-nuclear-science platform [5]. The burner, at $Q_E = 1.318$ and $f_n = 5.44\%$, is quantitatively the neutron-lean converse: it sits within the advanced-fuel envelope mapped by Kulcinski and Santarius [19] and Nevins [20], respects Rider's warning about non-equilibrium recovery by keeping the plasma near-Maxwellian and paying the recirculation honestly (equation 14) [21], and reproduces the WHAM-class Pastukhov-plug operating point [18].

WHY THE FLYWHEEL IS THE LOAD-BEARING RESULT

The most consequential number in the paper is not a gain but a time constant. Equations (9)–(10) show that the helium-3 co-product is governed by the $\tau = 17.8\,yr$ decay of banked tritium, and equation (12) turns that slowness into the flat statement of figure 5: $45–192$ breeders would be needed to fuel one burner from indigenous decay. This is why the platform's helium-3 is a strategic *co-product* and burner-scale fuel is *lunar-gated* [23,24]—a conclusion that falls straight out of the half-life and is robust to every plausible breeding assumption, since even the 1.42 ceiling needs ≈ 85. The honest framing throughout is that helium-3 value is not helium-3 revenue and the loop does not close between the two machines; the fuel-cycle companion carries the full indigenous-non-closure case (doi:10.5281/zenodo.22645734).

TWO MAGNETS, ONE BASIS

A recurring source of confusion in compact high-field concepts is the magnet. The platform shares a REBCO *basis*—no-insulation coated conductor, demountable practice, quench-margin methodology—but uses two *distinct* magnets: the 16.84 T breeder centrepost and the 26.49 T burner plug coil (figure 8). Both sit within demonstrated REBCO field practice [8], but they are different devices with different load lines, and the platform's magnet-integrity case depends on never conflating them.

§ 9

Limitations

One honest gate bounds the burner side of the platform. The burner's engineering gain $Q_E = 1.318$ closes on model with $P(Q_E > 1) = 1.0$ over the sampled envelope, but its one residual *physics* gate is the plug potential: the requirement $n_p/n_c = 16$ (equation 13) is a density-ratio target that a plug-scale potential experiment must demonstrate at the operating T_e, and the $40{,}000$-sample uncertainty quantification fixes the plug density and excludes central-cell radial transport (`KX–L1–A5–BU`). The magnet is *not* the gate—the 26.49 T plug coil qualifies structurally (doi:10.5281/zenodo.22645915)—and the flywheel result is a closed-form consequence of a measured half-life. The distance from closed-on-model to closed-demonstrated for the burner is therefore one named experiment, the plug-potential demonstration, not open physics.

§ 10

Conclusion

Kronos is one platform with two machines and a single frozen physics record. The breeder is a compact negative-triangularity spherical tokamak at $Q = 3.076$ and $P_{\text{fus}} = 85.04\,MW$ that makes strategic materials—tritium along a net breeding ladder to a 1.42 ceiling (clearing self-sufficiency at 1.05), helium-3, 14 MeV neutrons, and co-produced isotopes—behind a 16.84 T centrepost. The burner is a D–^{3}He tandem mirror at $Q_E = 1.318$ and a neutron energy fraction of 5.44%, recovering charged-particle power at $\eta_{\text{DEC}} = 0.49$ behind a distinct 26.49 T plug coil. Linking them is the helium-3 flywheel, whose governing balance (equations 8–10) shows that banked tritium discharges to helium-3 over an e-folding time of $17.8\,yr$—slow enough that indigenous helium-3 cannot fuel a burner fleet (equation 12; figure 5), which is why burner-scale fuel is lunar-gated and the breeder's helium-3 is a strategic co-product rather than bulk fuel. Stated in two tiers: all three products close on the frozen physics, every component is buildable within demonstrated REBCO and mirror practice, and the distance to demonstrated closure is a small number of named experiments—the measured breeding ratio at first-of-a-kind operation and the plug-potential demonstration—not open physics.

Acknowledgments tocsectionAcknowledgments Part of the Kronos Fusion Energy 2026 design series. The author thanks the Kronos physics de-risking programme for the frozen result set underlying every quantitative claim, and the NVIDIA GPU high-performance-computing campaign that produced and independently re-ran it.

Reproducibility. Every headline quantity in this paper is a frozen anchor in the Kronos Physics De-Risking Register [25] (doi:10.5281/zenodo.22133057), quoted inline by serial. The flywheel model (equations 8–10), the surplus law (7) and the fleet ratio (12) are regenerable from the archived toolkit and the figure-generation script deposited with this paper; the breeding ladder and burner uncertainty quantification are regenerable from the archived OpenMC and toolkit inputs. This paper is archived at doi:10.5281/zenodo.22645764; official version: https://www.kronosfusionenergy.com/publications/integrated-platform-overview.html.

Scope — what this paper does not claim. No product is claimed *demonstrated*-closed; each closes on model, with the distance to demonstrated closure stated as named experiments. No economic, cost, or valuation content appears anywhere in this paper, by design.

Data availability tocsectionData availability The reactivity, breeding-ladder, flywheel, fleet-ratio, plug-potential and burner-uncertainty data plotted in figures 2–6 and 7–8 are archived with the deposit at doi:10.5281/zenodo.22645764, which references the Kronos 2026 series including the tritium-breeding (doi:10.5281/zenodo.22645746), net-TBR fleet (doi:10.5281/zenodo.22645706), helium-3 fuel-cycle (doi:10.5281/zenodo.22645734), burner power-balance (doi:10.5281/zenodo.22645860) and plug-coil (doi:10.5281/zenodo.22645915) companions. All quantitative values trace to the register [25] by the serial identifiers cited inline.

Competing interests tocsectionCompeting interests Provisional patent applications relating to aspects of this work have been filed.

tocsectionReferences

APPARATUS

Portfolio, People & Record

The intellectual-property estate, the people who built it, the limitations that gate it, and the sources it rests on.

1	4	40	27
GRANTED PATENT	2026 PROVISIONALS	TEAM MEMBERS	2022 PROVISIONALS

INTELLECTUAL PROPERTY

The patent portfolio

The estate spans a granted high-field magnet patent, pending utility and 2026 provisional filings that map to the two products, a digital-twin control provisional, a registered trademark application, and the original 2022 provisional family. Every patentable disclosure in the five-paper arXiv drop was protected **before** publication: the breeder and burner provisionals were filed 1–2 August, and a publication-gap omnibus filing the evening before the drop swept up the DEC, plasma-control, and REBCO-winding matter of the three otherwise-unprotected papers. Patent numbers and application serials are matters of public record; claim scope is summarised, not reproduced.

GRANTED & PENDING UTILITY

US 12,009,112	High-field tilted graded-REBCO magnet architecture (KRONO-002A) · *app. 17/878,550*	GRANTED
US 17/878,507	Core device / method (KRONO-001A) · *utility*	PENDING

2026 PROVISIONAL FILINGS — MAPPED TO THE PRODUCTS

64/124,209	Hyperion — spherical-tokamak tritium / helium-3 foundry · *breeder · filed Aug 2026*	FILED
64/124,220	Aegis / MetroVolt — synchrotron-cutoff, fuel-selection & plug-winding · *generator · filed Aug 2026*	FILED
64/115,167	KRONOS-CTRL digital-twin plant control · *provisional · filed Jul 2026*	FILED
64/005,440	Integrated spherical-tokamak fusion architecture · *early integrated-architecture filing · filed Mar 2026*	FILED
64/105,530	Negative-triangularity spherical-tokamak architecture · *foundational ST filing · filed Jul 2026*	FILED
64/128,097	Publication-gap omnibus — quasineutral two-species expander DEC · provenance-gated / latency-split plasma control · as-built high-field winding & conductor architecture · *filed 7 Aug 2026, the evening before the arXiv drop*	FILED

TRADEMARK & ORIGIN

FTK-98801894	Kronos Fusion Energy — trademark application	FILED
KR-2022-*	Original provisional family (KR-2022-00001 … 00027) · *27 filings, 2022*	PRIORITY

The narrow, defensible magnet novelty — the specific conductor and the digital-twin winding optimisation, not high-field REBCO as a category — is the commercial core that can earn ahead of any Q > 1 milestone, with markets in fusion magnet supply, MRI/NMR, accelerators, and proton therapy. The claim is scoped honestly: the high field is a *system field* result, not a stand-alone-coil record; the small-bore plug coil is structurally infeasible as a bare winding but resolved by a stress-managed structural shield (feasible-pending-FEA); and the winding-tape experiment returned a *null result*. The value is the method, not a field record.

THE TEAM

Founding partners, board, advisors & auditors

Kronos is built by a bench of advanced-fuel-fusion, high-field-magnet, direct-conversion, and materials specialists, with a board and operations team drawn from defense, national laboratories, and industry. Dates are shown as ranges; where a tenure has ended or is term-ending, the range says so.

FOUNDING PARTNERS — SCIENCE

Dr. Gerald Kulcinski
Co-Founder · Helium-3 & Advanced-Fuel Fusion
UW–Madison · 2023–Present

Dr. Carl Weggel
Chief Scientist / S.M.A.R.T. Design
MIT Alcator Program · 2022–Present

Dr. Robert J. Weggel
Magnetic Field Design
MIT Magnet Lab · 2022–Present

BOARD

Priyanca Ford
Founder & CEO · Executive Board
2022–Present

Bandel Carano
Finance / Strategy
Oak Investment Partners / Stanford · 2025–2026

Patrick Schweiger
Fusion Device Engineering
Oklo / CFS / TerraPower · 2025–Present

SCIENTIFIC ADVISORS

Dr. Steven O. Dean
Fusion Policy & History
DOE / Fusion Power Associates · 2025–Present

Dr. Patrick H. Diamond
Plasma Turbulence & Transport
UC San Diego · 2025–Present

Dr. Jack J. Dongarra
HPC & Numerical Algorithms
Turing Award · 2025–Present

Dr. Nasr M. Ghoniem
Chief Material Scientist
UCLA · 2025–Present

Dr. Siegfried Glenzer
Plasma Physics & Laser Fusion
Stanford / SLAC · 2022–Present

Dr. David A. Hammer
Pulsed-Power Fusion
Cornell · 2025–Present

Dr. Donald A. Spong
Plasma Theory & Confinement
ORNL · 2025–Present

Dr. Curtis Smith
Risk Assessment & Nuclear PRA
MIT / Idaho National Lab · 2025–Present

RADM (Ret.) David Goggins
Naval Engineering & Power-Plant Design
U.S. Navy · 2023–2026

Dr. Konstantin Batygin
Mathematician
Caltech · 2022–2025

Dr. Ruben Fair
Magnet Design / ITER Liaison
PPPL / Jefferson Lab · 2022–2025

Dr. Paul S. Weiss
Materials & Nanotechnology
UCLA · 2022–2025

SCIENTIFIC AUDITORS

Dr. Wilfred A. Cooper
Plasma Equilibrium Theory
EPFL / Swiss Plasma Center · 2025–Present

Dr. Ahmed Hassanein
Plasma–Material Interactions
Purdue / Argonne · 2025–Present

Dr. Patrick E. Hopkins
Extreme Thermal Materials
U. of Virginia · 2025–Present

Dr. Peter Hosemann
Materials Joining & Structural Integrity
UC Berkeley · 2025–Present

Dr. Travis W. Knight
Advanced Nuclear Fuels & Systems
U. of South Carolina · 2025–Present

Dr. Philippe Lebrun
Cryogenics & Magnet Cooling
CERN · 2025–Present

Dr. Nitendra Singh
Nuclear Safety & Fuel Cycle
ITER · 2025–Present

Dr. Guido Van Oost
Magnetic Confinement & Fusion Systems
Ghent University · 2025–Present

Dr. Gary S. Was
Radiation Materials & Structural Integrity
U. of Michigan · 2025–Present

Dr. Ray Sedwick
Direct Energy Conversion
U. of Maryland · 2025

OPERATIONS

Michael Laughlin
Chief Operating Officer
2022–Present

Martin Owens
Chief Strategy Officer
LANL / GE Hitachi · 2022–Present

MG (Ret.) Paul Pardew
Chief Contracting Officer
Army Contracting Command · 2022–Present

David Beck
Fusion Commercialization
U.S. Space Force · 2024–Present

Sushma Bhatia
Environmental & Legislative
Google · 2022–Present

Michael De Frenza
Technology Licensing
2023–Present

MG (Ret.) Robin L. Fontes
Cybersecurity & Defense
Army Cyber Command · 2022–Present

Vijay Gehani
Supply Chain & Components
INOX India · 2024–Present

Jon Michel Greenwood
IT & AI Infrastructure
Live Nation · 2023–Present

Brian C. O'Neill
National Security
CIA / ODNI · 2022–Present

Gen. (Ret.) Gustave F. Perna
DoD Liaison
Operation Warp Speed · 2022–2023

Andrea Romero
Marketing Lead
2022–Present

Legal counsel is retained; those roles are held on the internal roster and are not listed here.

SOURCES

References

1 J D Lawson, Some criteria for a power producing thermonuclear reactor, *Proc. Phys. Soc. B* **70** 6 (1957). doi:10.1088/0370-1301/70/1/303

2 ITER Physics Expert Groups, ITER Physics Basis, Chapter 1: Overview and summary, *Nucl. Fusion* **39** 2137 (1999). doi:10.1088/0029-5515/39/12/301

3 H-S Bosch and G M Hale, Improved formulas for fusion cross-sections and thermal reactivities, *Nucl. Fusion* **32** 611 (1992). doi:10.1088/0029-5515/32/4/I07

4 M Greenwald *et al*, A new look at density limits in tokamaks, *Nucl. Fusion* **28** 2199 (1988). doi:10.1088/0029-5515/28/12/009

5 J E Menard *et al*, Fusion nuclear science facilities and pilot plants based on the spherical tokamak, *Nucl. Fusion* **56** 106023 (2016). doi:10.1088/0029-5515/56/10/106023

6 B N Sorbom *et al*, ARC: a compact, high-field, fusion nuclear science facility and demonstration power plant with demountable magnets, *Fusion Eng. Des.* **100** 378 (2015). doi:10.1016/j.fusengdes.2015.07.008

7 A J Creely *et al*, Overview of the SPARC tokamak, *J. Plasma Phys.* **86** 865860502 (2020). doi:10.1017/S0022377820001257

8 S Hahn *et al*, 45.5-tesla direct-current magnetic field generated with a high-temperature superconducting magnet, *Nature* **570** 496 (2019). doi:10.1038/s41586-019-1293-1

9 M E Austin *et al*, Achievement of reactor-relevant performance in negative triangularity shape in the DIII-D tokamak, *Phys. Rev. Lett.* **122** 115001 (2019). doi:10.1103/PhysRevLett.122.115001

10 A Marinoni, O Sauter and S Coda, A brief history of negative triangularity tokamak plasmas, *Rev. Mod. Plasma Phys.* **5** 6 (2021). doi:10.1007/s41614-021-00054-0

11 M Abdou *et al*, Physics and technology considerations for the deuterium–tritium fuel cycle and conditions for tritium fuel self sufficiency, *Nucl. Fusion* **61** 013001 (2021). doi:10.1088/1741-4326/abbf35

12 P K Romano, N E Horelik, B R Herman, A G Nelson, B Forget and K Smith, OpenMC: a state-of-the-art Monte Carlo code for research and development, *Ann. Nucl. Energy* **82** 90 (2015). doi:10.1016/j.anucene.2014.07.048

13 J Candy, E A Belli and R V Bravenec, A high-accuracy Eulerian gyrokinetic solver for collisional plasmas, *J. Comput. Phys.* **324** 73 (2016). doi:10.1016/j.jcp.2016.07.039

14 V P Pastukhov, Collisional losses of electrons from an adiabatic trap in a plasma with a positive potential, *Nucl. Fusion* **14** 3 (1974). doi:10.1088/0029-5515/14/1/001

15 T K Fowler and B G Logan, The tandem mirror reactor, *Comments Plasma Phys. Control. Fusion* **2** 167 (1977).

16 G I Dimov, V V Zakaidakov and M E Kishinevsky, Thermonuclear confinement with twin mirror systems, *Sov. J. Plasma Phys.* **2** 326 (1976).

17 R F Post, The magnetic mirror approach to fusion, *Nucl. Fusion* **27** 1579 (1987). doi:10.1088/0029-5515/27/10/001

18 D Endrizzi *et al*, Physics basis for the Wisconsin HTS Axisymmetric Mirror (WHAM), *J. Plasma Phys.* **89** 975890501 (2023). doi:10.1017/S0022377823000806

19 G L Kulcinski and J F Santarius, Advanced fuels under debate, *Nature* **396** 724 (1998). doi:10.1038/25456

20 W M Nevins, A review of confinement requirements for advanced fuels, *J. Fusion Energy* **17** 25 (1998). doi:10.1023/A:1022513215080

21 T H Rider, Fundamental limitations on plasma fusion systems not in thermodynamic equilibrium, *Phys. Plasmas* **4** 1039 (1997). doi:10.1063/1.872556

22 R W Moir and W L Barr, “Venetian-blind” direct energy converter for fusion reactors, *Nucl. Fusion* **13** 35 (1973). doi:10.1088/0029-5515/13/1/005

23 L J Wittenberg, J F Santarius and G L Kulcinski, Lunar source of ^{3}He for commercial fusion power, *Fusion Technol.* **10** 167 (1986). doi:10.13182/FST86-A24972

COLOPHON

How this document was made

The Kronos Fleet — Combined Editorial, 2026 is set in **Fraunces** (display), **Gelasio** (text), and **IBM Plex Mono** (data & equations), carried forward from the Kronos editorial design system.

The figures are rendered at 300 dpi from the deposited generator scripts; the document is composed as a single self-contained file with embedded fonts and imagery, paginated to US Letter, and rendered to PDF through a headless Chromium engine in matched light and dark editions.

Every headline quantity carries an evidence class; withdrawn and restated values are marked as such. Nothing herein is frozen beyond the founder-approved Tier-A set.

Explore it live — turn the interactive 3-D model, run the deposited solvers in the physics validator, and watch the companion film series.

LEGAL NOTICE

Notice, status, and distribution

Conceptual design & simulation study. This document reports a conceptual design and simulation study. It is not a construction commitment, a safety-analysis report, a regulatory filing, or an offer of securities. Forward-looking statements — schedules, costs, market sizes, and performance — are estimates subject to the limitations set out in the Simulations part and may change.

Numbers and their classes. Quantities are reported with evidence classes and case labels; modelled, assumed, and requirement-class values are identified as such and are not to be quoted without their labels.

Public edition. This edition carries the physics and design only; all financial, funding, and defense-commercial content has been removed for public distribution. The scientific text corresponds to the arXiv and journal submissions.

THE 2026 KRONOS SERIES

One programme, many papers

This editorial is one paper in the Kronos 2026 series — a real fusion company's complete, reproducible physics record for a spherical-tokamak breeder and its low-neutron D–^{3}He tandem-mirror burners. Every headline number is a frozen anchor in the Physics De-Risking Register.

Explore the whole programme: the De-Risking Register, the interactive 3-D model, and the physics validator.

KRONOS FUSION ENERGY

The Kronos Strategic-Materials Platform: An Integrated Spherical-Tokamak Breeder and D-3He Tandem-Mirror Burner Architecture with a Helium-3 Flywheel

A real fusion company building real machines. Explore the science, live.

Zenodo · doi:10.5281/zenodo.22645764

Read on kronosfusionenergy.com

The Physics De-Risking Register